UHF RFID Wireless Communication System for Real Time ECG Monitoring

Md. Moklesur Rahman, Toufiq Aziz and Heung-Gyoon Ryu
Department of Electronic Engineering, Chungbuk National University,
Cheongju 28644, Korea
m.moklesur.r@gmail.com, toufiqaziz.dream@gmail.com and ecomm@cbu.ac.kr

Abstract **– Electronic Health Records (EHR) and monitoring are very essential and nowadays, a large number of Internet of Things (IoT) health care devices are available but it has still difficulties to log the real time patient monitoring like heart rate variability (HRV) in the healthcare checkup center. Generally, heart rate variability (HRV) is widely assumed for evaluating the health condition of human. One of the best ways to observe the heart rate variability (HVR) information is the Electrocardiograms (ECG) for that the wired manner is the ordinary approach. Even though any wireless ECG system was suggested, the low accuracy, very short service range and the limited battery life are the major drawbacks. So, in this paper, we like to propose a new Ultra High Frequency (UHF) Radio Frequency Identification (RFID) communication system to monitor ECG signals about the heart activities. The system is designed based on the ESPAR (electronically steerable parasitic array radiator) antenna to make a beamforming to the direction of the RFID tag containing ECG sensor. Also, this paper investigates the distance between the sensor tag and the RFID reader to improve the link budget of the UHF-RFID system. Finally, it is demonstrated that the range is longer higher than the previously results.**

Keywords – UHF, RFID Reader, ECG, ESPAR antenna, Link Budget, Range.

I. INTRODUCTION

There are many commercially available health monitoring kits. Among them ECG (Electrocardiograms) is a remarkable innovative invention in the Biomedical sector. These devices more commonly use a photoplethysmogram (PPG) sensor to provide a semi-accurate heart rate reading for sports and others well-being applications. More advanced systems employ a strap-based system which can utilize an ECG chip to monitor the heart [1] which is capable of monitoring a patient patient's heart rhythms for 24 to 48 hours during normal human activity [2-3].

Applications of Radio Frequency Identification (RFID) systems have greatly facilitated the supply-chain and logistics industry. During the past couple of years, the passive RFID systems operating in the Ultra-High Frequency (UHF) band are especially attractive due to their significant advantages such as long identification range, low cost and small size. Passive tag is typically composed of an antenna and an integrated circuit chip. It acquires power entirely from the impinging electromagnetic fields radiated by an RFID reader. In order to send information back to the reader, the tag modulates the backscattered fields by varying its antenna load [4]. Also, the emerging RFID technology has brought new opportunities for HRV monitoring in a more convenient and accurate approach, as the RFID tag can be regarded as an extremely lightweight sensor and its nature of identification can be used to effectively and easily distinguish different human subjects.

In wireless communication systems, the received power is an important parameter since sufficient power is necessary to maintain a given set of data exchange [5]. Radio link budget generally refers to the expression for prediction of received power, and it is a determinant factor for the coverage estimation. We can roughly estimate the coverage range by means of combining radio link budget with other parameters, such as the sensitivity of the receiver and transmitted power of the transceiver [4].

In this paper, we like to propose a new UHF RFID communication system to monitor ECG signals about the heart activities. The system is designed based on the ESPAR antenna to make a beamforming to the direction of the RFID tag containing ECG sensor. ESPAR is the technique by which beam steering is achieved without the use of phase shifters. In ESPAR antenna, a driven element is surrounded by closely spaced parasitic elements. The distance between the sensor tag and the RFID reader is investigated to improve the link budget of the UHF-RFID system.

II. SYSTEM DESIGN

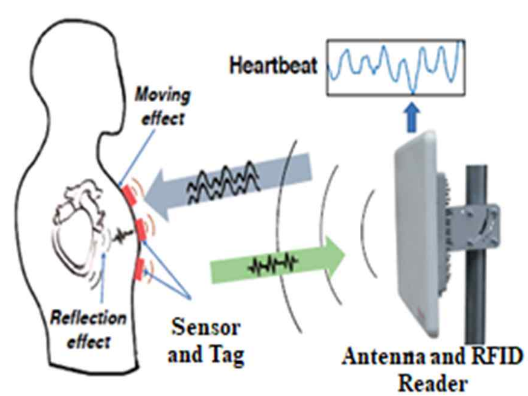

Fig.1. UHF RFID communication diagram for ECG monitoring.

Fig.1 shows the proposed UHF RFID communication diagram for ECG monitoring. To enable UHF RFID communications the EM4325 made by EM microelectronic can be used, as it has been previously utilized in streaming higher data rate body-centric data [7] and was shown to reliably stream accelerometer data [1]. The EM4325 could be chosen because of the RAM register access through SPI cable. The majority of commercially available the UHF RFID chips have memory access as a standard feature. The EM4325 has also ability to change its transmission characteristics depending on the external power [8], two power modes for transmission are commonly used, one which relies on the power harvested from the reader, and another which uses a small amount of power from an external battery [1]. The ESPAR antenna used for the design utilized to enable an efficient interface to the EM4325. The design circuit must such that there will be sufficient spacing around the antenna edge to give the highest performance.

To observe ECG waveform, the microchip MAX30001 can suitably be selected due to its low power performance and small package. The chip requires minimal external circuitry which enabled the design to be compact in order to conform within the design specifications of the antenna [1]. Low energy microcontroller TI CC2640R2 BLE Module [li2018] could also be the suitable candidate in the proposed design system.

Embedded Processing process and forward the incoming data between the ECG sensor and the communications chip, the Texas Instruments MSP430FR5969 microcontroller is usually used. From the data sheet it is obtained the power management of this microcontroller is focused heavily on the wake states, but also provides extremely low power consumption during sleep states. The microcontroller uses a main SPI bus to interface all of the communicating devices, ensuring minimal signal traces. During peak operation the microcontroller uses up to 1.6 mA (at full speed), and can be cycled into a low power sleep mode which consumes 0.02 μA.

To enable the device to be functioned properly, exact power management is very important that is why a small lithium Polymer battery (120mAh) could be employed, with a charging and regulation stage used. The charging stage is a MCP7381T-2ACI, which allowed for external power to be applied between the charge phase and regulation phase to recharge (fill up) the battery. The regulation phase used a ADP1710 which regulate the voltage to a system wide 2V.

III. Link Budget Analysis

Using the Friis equation, the expected received power by an RFID reader can be mathematically expressed as [9],

$$P_{r,tag}\,(dB_m) = P_{reader}\,(dB_m) + G_{reader}\,(dB) + G_{tag}\,(dB) + 10bg_{10}\,(1-|\rho|^2) + \Delta G\,(dB) - L_{sys}(dB) - L_p\,(dB) \quad (1)$$

where P_{reader} is the transmitted power by the reader, G_{reader} and the G_{tag} are the gains of the reader and tag, ρ is the reflection coefficient of the tag, ΔG represents the gain penalty when the tag is on contact, L_{sys} is the cable loss or system loss, L_p is the path loss.

When the power received by the reader, the backscatter communication radio link budget $P_{r,tag}$ (dB_m) can be written as

$$P_{r,tag}\,(dB_m) = P_{reader}\,(dB_m) + 2G_{reader}\,(dB) - L_{sys}\,(dB) + 10bg_{10}\frac{RCS}{4\pi} + 20bg_{10}\frac{\lambda}{4\pi} - 40bg_{10}\,(r) \quad (2)$$

Where r is the distance between tag and reader, λ is the wavelength; RCS stands for radar cross section (RCS) of the tag. The modulated backscattered signal is proportional to the antenna mode of the RCS and can be written as a function of the antenna gain [4], [9].

$$RCS = G^2\lambda^2\rho_0^2/4\pi \quad (3)$$

Here, ρ_0^2 is the differential reflection coefficient of the tag $\rho_0^2 = |\rho_1 - \rho_2|$; ρ_1 and ρ_2 are on the 0 and 1 states of the chip's reflection coefficient.

The gain penalty factor ΔG is introduced to take into account the change in the antenna gain and impedance [10]. Due to the material change, ΔG represented as

$$\Delta G = G_{tag,\ material}\,(dB) - G_{tag,\ free\ space}\,(dB) \quad (4)$$

Therefore, the power received in the tag is given by

$$P_{r,tag}\,(dB_m) = P_{reader}\,(dB_m) + 2G_{reader}\,(dB) + 2G_{tag}\,(dB) + 20bg_{10}\,(\rho_0) + 2\Delta G\,(dB) - 2L_{sys}(dB) - 2L_p\,(dB). \quad (5)$$

Although RFID is a line of sight (LOS) communication system [11], the influence of reflections in the environment must be considered. Path loss from equations (1) and (5) can be modeled as the sum of several waves reflected in ground, hills, walls or other objects. Thus, we have

$$L_p = -20bg_{10}\left(\frac{\lambda}{4\pi}\right)^2 - 20bg_{10}\left[\frac{e^{-jkr_0}}{r_0} + \sum_{i=1}^{N}\Gamma_i\sqrt{t_i}\,\frac{e^{-jkr_i}}{r_i}\right] \quad (6)$$

Where r_0 is the direct path length, r_i is the length of the ith reflected ray path, N is the total number of reflections and k is the wave number, t_i is the normalized antenna radiation pattern, Γ_i is the Fresnel's reflection coefficient. Only for the direct path r_o, the path loss, L_p implied as

$$L_p = -20bg_{10}\left(\frac{\lambda}{4\pi}\right)^2 - 20bg_{10}\left(\frac{e^{-jkr_o}}{r_o}\right) \quad (7)$$

Again, only when the direct path is considered, equation (6) reduces to free-space Friis model. Another simple model takes into account such as direct ray and reflection in the ground [16], assuming the flat earth model, N=1. In this case, the distance between tag-reader is larger than antenna height h_1, h_2 ($r \gg \frac{4h1\,h2}{\lambda}$) and the Γ_i is almost real and the worst when $\Gamma_i = -1$, the path loss when flat earth model is considered can be written as

$$L_p = -10\,bg_{10}\left[\frac{(h1h2)^2)}{r^4}\right] \quad (8)$$

An empirical model is often used in the indoor environments such as RFID. The path loss is based on slope model [16].

$$L_p = - 20 bg_{10} (\frac{\lambda}{4\pi}) + n * 10 * bg_{10} (r) \quad (9)$$

Where n is the path loss factor for distances shorter than the turn-on distance in RFID system. For fee space n= 2.

IV. ESPAR ANTENNA AND RANGE EXTENSION

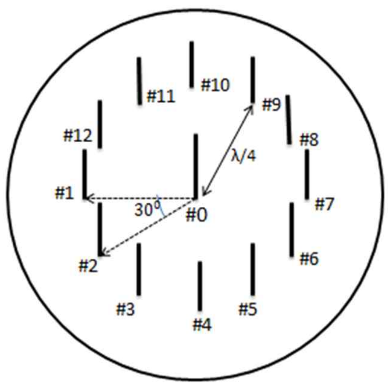

Fig. 2. Structure of 13-elements ESPAR antenna.

The ESPAR antenna is designed with the CST 3D Electro-magnetic Simulator. It consists of one active monopole (numbered as #0) placed in the center of the metal ground plane surrounded by 12- parasitic elements (numbered as #1- #12) printed on Rogers RO4725-JXR dielectric substrate. It has a thickness of h = 0.787 mm and it exhibits a relative permittivity of ε_r = 2.55, so the antenna can be used in inexpensive in our proposed system.

The thickness of the ground is 0.035mm. To design low-profile ESPAR antenna that it has significantly reduced height when compared to [12,13] , the original concepts while its radiation patterns can successfully be used to provide accurate direction of arrival (DoA) estimation, a number of constructions based on microstrip radiators has been investigated [14]. The active monopole is fed by the coaxial connector via the central pin in order to provide 50Ω impedance appropriately. The parasitic elements can be opened (directors that pass through the electromagnetic wave) or shortened (reflectors that reflects the energy) to the ground by the pin diode switching circuits designed on dielectric substrate. The central pin of every surrounding passive elements can be connected to the ground via a corresponding switching circuit realized using SMP1320-040LF PIN diode. The close distance (λ/4) between each parasitic elements and the active printed monopole causes strong mutual coupling effects and provides a reconfigurable radiation pattern to the ESPAR antenna according to which parasitic monopole is connected to the ground plane [15].

The complete polar radiation pattern for two different configurations of the proposed antenna at 2.40 GHz for various steering vectors, V_{max}^{n} (i.e. V_{max}^{1} , $V_{max}^{2}, V_{max}^{3} \dots , V_{max}^{12}$) and for beam direction, φ_{max}^{n} = 0^0, 90^0 on the xz- plane are illustrated in the Fig. 3 and 4.

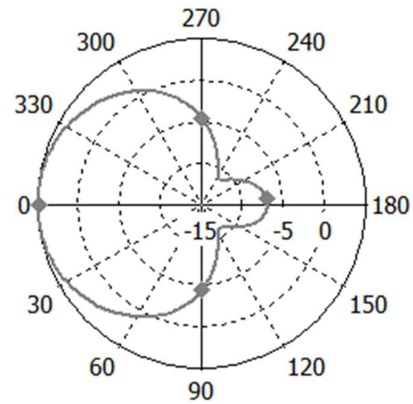

Fig.3. Simulation polar radiation pattern of the proposed antenna at 2.40 GHz for φ_{max}^{1}= 0^0.

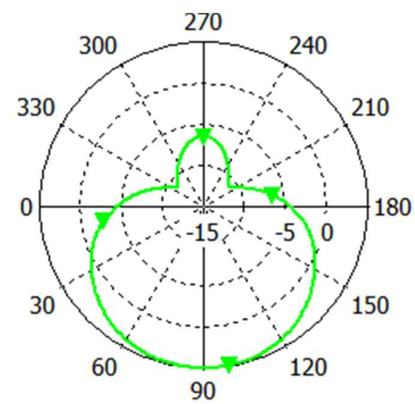

Fig. 4. Simulation polar radiation pattern of the proposed antenna at 2.40 GHz for φ_{max}^{2}= 90^0.

The link margin, L_m, informs about how much margin there is on the communication link before starting to get packet errors,

$$L_m = P_{r,tag} (dB_m) - S_r (dB_m); \quad (L_m>0) \quad (10)$$

Here, S_r (dB_m) is the $P_{r,tag}$ (dB_m) Sensitivity. Absolute maximum range can be calculated by setting the link margin to 0.

$$L_m = P_{r,tag} (dB_m) - S_r (dB_m) = 0 \quad (11)$$

For 2.40 GHz frequency the path loss, L_p can be represented by,

$$L_p = - 40 + 2 * 10 * bg_{10} (r) \quad (12)$$

Equation (5) can be written as

$$P_{r,tag} (dB_m) = P_{reader} (dB_m) + 2G_{reader} (dB) + 2G_{tag} (dB) + 20 bg_{10} \rho_0 + 2\Delta G (dB) + 2L_{sys}(dB) + 2L_p (dB) \quad (13)$$

It is important to keep in mind is that the loss terms here are written as positive but at the time of substituting values these will be negative as they can never be greater than 0 dB. The constant values to obtain the range based on the above equations are listed in table 1.

TABLE I. PARAMETERS FOR COMMUNICATION RANGE AT 2.40 GHZ

Parameters	value
Frequency	2.40 GHz
Reader antenna power, P_{reader}	24 dB
Reader antenna gain, G_{reader}	8.44 dB
Tag antenna gain, G_{tag}	8.44 dB
Reflection coefficient, ρ_o	1 dB
Gain penalty, ΔG	0 dB
System loss, L_{sys}	- 5 dB
Path loss, L_p	- 40dB, - 60 dB, -75 dB
Sensitivity, S_r	- 105 dB
Path loss factor, n	2
Link margin, L_m	0 dB

When the path loss, L_p = -40 dB the distance between the transmitter and the receiver, r = 1 meter or 100 centimeter. At the same time the power received by the tag, $P_{r,tag}$ = - 32.24 dB. In the same way, when L_p = -60 dB, - 75 dB, the distance, r= 10 centimeter, and 1.8 centimeter. Both cases the power received by tag $P_{r,tag}$ = - 72.24 dB and -102.24 dB. The link margin, L_m for the three received power by tag are as follows,

$$L_m = P_{r,tag}\,(dBm) - S_r\,(dBm) = -32.24 - (-105) = 72.76\ dB.$$

Similarly, L_m is equal to 32.76 dBm and 2.76 dB. If the path loss, L_p = - 30 dB, the distance between the RFID tag and the RFID reader, r = 3.162 meter.

VI. CONCLUSIONS

In this paper, we have proposed a new Ultra High Frequency (UHF) Radio Frequency Identification (RFID) wireless system to monitor heart activities. The beam steering exhibits very high performance regarding radiation pattern, gain, and the reflection coefficient. The range based on the link margin in calculated and represented that it shows well results at the path loss of the -60 dB, where the distance between sensor tag and antenna RFID Reader is 10 centimeter (cm) and the link margin is 32.76 dB. From which it is demonstrated that the range is higher than the previously published ones papers. Thus, the proposed design is considered to be a reliable, robust, relatively long distance, and low-power-transmission (longer distance) ECG monitoring system.

ACKNOWLEDGMENTS

This work was supported by the National Research Foundation of Korea (NRF) grant funded by the Korea government (Ministry of Education) (NRF-2016R1D1A1B01008046) and this work was supported under the framework of international cooperation program managed by the National Research Foundation of Korea (2019K1A3A1A3910299511, FY2019). Also, this work was supported under the framework of international cooperation program managed by the National Research Foundation of Korea (2020K2A9A2A08000106, FY2020).

REFERENCES

[1] Robert Horne, John Batchelor, Paul Taylor, Ertan Balaban and Alex Casson, “Ultra-Low Power on Skin ECG using RFID Communication,” 2020 IEEE International Conference on FLEPS, Manchester, UK, 16-19 Aug. 2020.

[2] Amit Walinjkar* and John Woods, “FHIR Tools for Healthcare Interoperability,” Biomedical Journal of Scientific & Technical Researc, Volume 9- Issue 5: 2018.

[3] Chuyu Wang, Lei Xie, Wei Wang, Yingying Chen, Yanling Bu, Sanglu Llu “RF-ECG: Heart Rate Variability Assessment Based on COTS RFID Tag Array,” Proc. ACM Interact. Mob. Wearable Ubiquitous Technol. 2, 2, Article 85, June 2018.

[4] Zhuo Su, Shing-Chi Cheung, Senior Member, IEEE, and Koon-Ting Chu, “Investigation of Radio Link Budget for UHF RFID Systems,” Program for the IEEE International Conference on RFID-Technology and Applications, 17 - 19 June 2010 Guangzhou, China June 2010.

[5] J.D. Griffin and G.D. Durgin, “Complete Link Budgets for Backscatter-Radio and RFID systems,” IEEE Antennas and Propagation Magazine, vol. 51, no. 2, pp. 11-25, April 2009.

[6] Cheng-Pin Wang, Shuenn-Yuh Lee and Wei-Chih Lai, “An RFID tag system-on-chip with wireless ECG monitoring for intelligent healthcare systems,” 2013 35th Annual International Conference of the IEEE Engineering in Medicine and Biology Society, 3-7 July 2013.

[7] R. Horne, P. Jones, P. Taylor, J. Batchelor, and C. Holt, “An on body accelerometer system for streaming therapy data using cots uhf rfid,” in 2019 IEEE International Conference on RFID Technology and Applications (RFID-TA), 2019, pp. 301–305.

[8] Robert Horne, John Batchelor, Paul Taylor, John Batchelor, Catherine Holt, “An On Body Accelerometer System for streaming therapy data using COTS UHF RFID,” 2019 IEEE International Conference on RFID-TA, Pisa, Italy, 2019.

[9] Antonio Lázaro, Member, IEEE, David Girbau, Member, IEEE, and David Salinas, “Radio Link Budgets for UHF RFID on Multipath Environments,” IEEE transactions on antennas and propagation, vol. 57, no. 4, April 2009.

[10] J. D. Griffin, G. D. Durgin, A. Haldi, and B. Kippelen, “RF tag antenna performance on various materials using radio link budgets,” IEEE Antennas Wireless Propag. Lett., vol. 5, pp. 247–250, 2006.

[11] P. V. Nikitin, K. V. S. Rao, and R. D. Martinez, “Differential RCS of RFID tag,” Inst. Elect. Eng. Electron. Lett., vol. 43, no. 8, pp. 431–432, Aug. 2007.

[12] K. Gyoda and T. Ohira, ``Design of electronically steerable passive array radiator (ESPAR) antennas," in Proc. IEEE Antennas Propag. Symp., Salt Lake City, UT, USA, vol. 2, , pp. 922_925, Jul. 2000.

[13] E. Taillefer, A. Hirata, and T. Ohira, ``Direction-of-arrival estimation using radiation power pattern with an ESPAR antenna," IEEE Trans. Antennas Propag., vol. 53, no. 2, pp. 678_684, Feb. 2005.

[14] Mateusz Burtowy, Mateusz Rzymowski , and Lukasz Kulas, “Low-Profile ESPAR Antenna for RSS-Based DoA,” IEEE. Translations and content mining are permitted for academic research only, Volume 7, 2019.

[15] Leonidas Marantis , Dimitrios Rongas, Anastasios Paraskevopoulos, Christos Oikonomopoulos- Zachos, Athanasios Kanatas, “Pattern reconfigurable ESPAR antenna for vehicle-to-vehicle communications,” IET Microw. Antennas Propag, Vol. 12 Iss. 3, pp. 280-286, 2018.

[16] R. Janaswamay, *Radiowave Propagation and Smart Antennas forWireless Communications*. Norwell, MA: Kluwer Academic, 2001.

[17] N. Ahmed, H, Rahman, and Md.I. Hussain, “A comparison of 802.11ah and 802.15.4 for IoT,” ICT Express, Vol.2, No. 3, Sep. 2016, pp. 100-102.

[18] Bin Liu, Zhisheng Yan, and Chang Wen Chen, "Medium Access Control for Wireless Body Area Networks with QoS Provisioning and Energy Efficient Design," IEEE Transactions on Mobile Computing, Vol. 16, No. 2, Feb. 2017, pp. 422-434.

[19] Muankid, Mahasak Ketcham, “The Real-time Electrocardiogram Signal Monitoring System in Wireless Sensor Network,” International Journal of Online and Biomedical Engineering (iJOE), Vol 15, No 02 (2019).

[20] Juyoung Park and Kyungtae Kang, “Intelligent Classification of Heartbeats for Automated Real-Time ECG Monitoring,” Telemedicine and e-HealthVol. 20, No. 12, 22 Dec 2014.

[21] Noh YH., Seo JY., Jeong DU, *Real-Time ECG Monitoring System Based on the Internet of Things Using an Optimum Transmission Technique.,* IT Convergence and Security 2017, Lecture Notes in Electrical Engineering, vol 450. Springer, Singapore.